



Science Arts & Métiers (SAM)

is an open access repository that collects the work of Arts et Métiers Institute of Technology researchers and makes it freely available over the web where possible.

This is an author-deposited version published in: <https://sam.ensam.eu>
Handle ID: <http://hdl.handle.net/10985/8355>

To cite this version :

Philippe STEYER, Kumar Ram MOHAN RAO, Denis LAGADRILLERE, Corinne NOUVEAU - Plasma Nitriding of 90CrMoV8 Tool Steel for the Enhancement of Hardness and Corrosion Resistance - Surface and Coatings Technology - Vol. 205, p.4514-4520 - 2011

Any correspondence concerning this service should be sent to the repository

Administrator : scienceouverte@ensam.eu



Plasma nitriding of 90CrMoV8 tool steel for the enhancement of hardness and corrosion resistance

Corinne Nouveau ^{a,*}, Philippe Steyer ^{b,2}, K. Ram Mohan Rao ^{a,1}, Denis Lagadrillere ^{c,3}

^a Laboratoire Bourguignon des Matériaux et Procédés (LaboMaP), Arts et Métiers ParisTech de Cluny, Rue Porte de Paris, F-71250, Cluny, France

^b Laboratoire MATEIS, Institut National des Sciences Appliquées de Lyon (INSA), 20, avenue Albert Einstein, F-69621, Villeurbanne Cedex, France

^c ARTS, Arts et Métiers ParisTech de Cluny, Rue Porte de Paris, F-71250, Cluny, France

A B S T R A C T

The aim of the study is to apply a plasma nitriding process to the 90CrMoV8 steel commonly employed in wood machining, and to determine its efficiency to improve both mechanical and electrochemical properties of the surface. Treatments were performed at a constant N₂:H₂ gas mixture and by varying the temperature and process duration. The structural and morphological properties of nitrided layers were characterized by X-ray diffraction (XRD) and scanning electron microscopy (SEM) coupled with EDS microanalyses. Surface hardening and hardness profiles were evaluated by micro hardness measurements. To simulate the wood machining conditions, electrochemical tests were carried out with an oak wood electrolyte with the purpose of understanding the effects of the nitriding treatment on the corrosion resistance of the tool in operation.

X-ray diffraction analyses revealed the presence of both γ' (Fe₄N) and ϵ (Fe₂₋₃N) nitrides with a predominance of the ϵ phase. Moreover, α -Fe (110), γ' and ϵ diffraction peaks were shifted to lower angles suggesting the development of compressive stresses in the post nitrided steel. As a result, it was shown that nitriding allowed a significant hardening of steel with hardness values higher than 1200 HV. The diffusion layers were always composed of an outer compound layer and a hardened bulk layer which thickness was half of the total diffusion layer one. No white layer was observed. Similarly, no traces of chromium nitrides were detected. The temperature seemed to be a parameter more influent than the process duration on the morphological properties of the nitrided layer, while it had no real influence on their crystallinity. Finally, the optimal nitriding conditions to obtain a thick and hard diffusion layer are 500 °C for 10 h.

On the other hand, to verify the effect of these parameters on the corrosion resistance, potentiodynamic polarization tests were carried out in an original "wood juice" electrolyte. After corrosion, surface was then observed at the SEM scale. Electrochemical study indicated that the untreated steel behaved as a passive material. Although the very noble character of steel was somewhat mitigated and the corrosion propensity increased for nitrided steels, the passive-like nature of the modified surface was preserved. For the same optimized parameters as those deduced from the mechanical characterization (500 °C, 10 h), surface presented, in addition to a huge surface hardening, a high corrosion resistance.

Keywords:

Plasma treatment

Alloy steel

Iron nitride

Surface modification

Hardness

Corrosion

1. Introduction

With the increasing need of wood furniture or wood based materials, there has been a corresponding increase in the importance of wood machining tools within the past decade [1]. In actual service conditions, these steel parts very often suffer from surface initiative degradations e.g. wear and corrosion. Degradation caused by wear in

operation was found to be very common for these materials, and a hardening of the surface was often proposed as a solution to improve its resistance. In addition, a high corrosion resistance was also required for a longer service life in aggressive media. Unfortunately, few efforts have been made to improve, simultaneously the corrosion and wear resistance. Nevertheless, enhanced tools had to fulfill this double-condition to meet the specific severe characteristics involved in wood machining. In the present work, an attempt is proposed to achieve both wear and corrosion resistance properties by modifying the surface of a wood-tool steel (90CrMoV8) by a plasma nitriding treatment.

Indeed, nitriding has been known for a long time to modify functional properties of the surface, regarding the mechanical, tribological, or electrochemical aspects. Different processes, based on diffusion of liquid [2] or gaseous states [3], have already proved

* Corresponding author. Tel.: +33 3 85 59 53 35; fax: +33 3 85 59 53 70.

E-mail addresses: nouveau@cluny.ensam.fr (C. Nouveau),

Philippe.Steyer@insa-lyon.fr (P. Steyer), rammohanrao.k@gmail.com (K.R. Mohan Rao), denis.lagadrillere@ensam.eu (D. Lagadrillere).

¹ Tel.: +33 3 85 59 53 53; fax: +33 3 85 59 53 70.

² Tel.: +33 4 72 43 81 69; fax: +33 4 72 43 87 15.

³ Tel.: +33 3 85 59 53 39; fax: +33 3 85 59 53 70.

their effectiveness. Physical vapor deposition can also be used for improving surface properties [4–6], but their application was often limited owing to poor adhesion of the coating [7].

Plasma processing gained substantial industrial development over the past several decades [8,9]. Amongst the several plasma based surface modification processes, plasma nitriding is considered as the most industrially adopted method [10,11]. In this process, parts are immersed in a nitrogen plasma environment, raised to a desirable temperature to facilitate diffusion of nitrogen into the bulk substrate until formation of the expected nitrides [12,13]. Advantages linked to plasma nitriding rest first on its versatility, coupled with its environmental-friendly aspects.

Previous studies focused on hardening of martensitic steel employing plasma nitriding showed promising effects. Chekour et al. [13] obtained high mechanical properties by nitriding 32CrMoV13 steel in various gas mixtures of nitrogen and hydrogen. Chala et al. [14] related that a top-coat of ZrBN deposited on plasma nitrided steel led to a significant enhancement of the corrosion resistance. Other approaches consisted in making the process more complex by adding further post-nitriding steps. As an example, post-oxidation or impregnation operations efficiently decreased porosities inside the nitrided layer, improving the corrosion protectiveness [15,16]. Plasma nitriding processes are also characterized by their low treatment temperatures [17]. In particular this advantage is of prime importance for stainless steels, for which the passive-ability inherent to high chromium contents may be lost by diffusion processes [18–20]. Gontijo et al. [21], for instance, indicated that treating 304 L stainless steels within the 450–500 °C temperature range preserved its original passive nature. In opposite, Nosei et al. [22] observed a decrease of corrosion resistance after plasma nitriding of 316 L stainless steel due to the formation of expanded austenite on its surface. For authors, this loss of passive-ability was due to an increase of the surface roughness prone to favor local dissolutions.

Unfortunately, the understanding of phenomena involved in the plasma nitriding of 90CrMoV8 steel, and especially its effects on mechanical and corrosion resistance properties, were still not fully explored. The aim of this study is not only the plasma nitriding of 90CrMoV8 steel but also to verify its opportunity to enhance both wear and corrosion resistances. If promising results are obtained, this innovative treatment could be applied in future works in wood machining. Then to correlate the microstructural and functional properties with the nitriding parameters, a metallurgical approach based on scanning electron microscopic observations coupled with microanalyses (EDS), X-ray diffraction analyses and micro hardness measurements were first adopted. Moreover, for the determination of the corrosion behavior of nitrided steels, electrochemical tests were performed in an original “wood juice” electrolyte susceptible to be oozed out when wood is machined.

2. Experimental part

2.1. Nitriding process

In the present study, 90CrMoV8 (“La Forézienne-MFLS” trademark, France) steel was plasma nitrided. The chemical composition of this steel is given in Table 1.

Sheets of the above steel (20 × 20 cm², 10 cm thick) were exposed to heat treatment at the austenite temperature, and then quenched in an

oil bath. Subsequently, the quenched samples were tempered at 530 °C. As a consequence, steel reaches the expected high hardness value of approximately 650 HV ± 30. Sheets were then cut into samples of 15 × 15 × 3 mm³ dimensions. These samples were subjected to metallographic polishing from coarse to fine SiC papers. Prior to nitriding, samples were cleaned for 20-min in an ultrasonic bath containing acetone, dried, and loaded into the nitriding furnace (BMI, Lyon-France). Characteristics of this reactor are described in previous studies [4,7]. The initial pressure was 0.5 Pa and the working pressure was 500 Pa. The typical cycle of the nitriding process began by an Ar etching performed at 800 Pa. Etching was maintained until the desired nitriding temperature was reached. Then, sputtering stops and nitriding process started for the desired duration. This nitriding process carried out in glow discharge plasma of a N₂ + H₂ gas mixture (80:20 ratio), the substrate holder was biased at –250 V. Once treatment is finished, treated parts are cooled down to room temperature.

Nitriding is a thermochemical process. Therefore, its efficiency is dependent on key-parameters linked to the diffusion: on the treatment temperature, the treatment duration and the gas mixture nature [23]. We decided to fix the gas mixture nature (N₂ + H₂ with a 80:20 ratio) and we focused our study on the effects of the two other parameters: therefore, treatments conducted for different times (from 6 to 12 h) at 500 °C and different temperatures (from 460 to 520 °C) during 10 h were realized, with the purpose of determining their influence on the mechanical and electrochemical properties of our steel.

2.2. Structural and mechanical characterizations

After nitriding, Vickers micro hardness tests (LECO MHT-210 micro hardness tester, 50 g applied load) were performed to assess the role of the treatment on the modification of the steel mechanical properties. Results correspond to the average of six measurements and the accuracy was 30 HV. Two hardness profiles were conducted on each sample for the reproducibility. SEM observations of the cross sections coupled with EDS microanalyses (SEM-Jeol JSM-5900, especially for the relative nitrogen amount) permitted to determine more precisely the chemical nature according to the nitriding parameters. The morphology and the diffusion layer structure of the nitrided layers were determined by cross section observations after etching of the material using Vilella's reagent. Finally, samples were characterized by XRD in order to identify the phases formed during the treatment (XRD – INEL CPS 120 diffractometer – $\theta/2\theta$ configuration using CoK α radiation source (0.17902 nm)).

2.3. Corrosion tests

In order to forecast the corrosion behavior of the nitrided steels in service conditions, electrochemical tests were performed in a specific original solution simulating the liquid oozed out during wood machining. This solution, called “wood juice”, was prepared by cutting oak wood to 5 × 5 mm² dimensions, crushing them, and then putting into suspension in distilled water. This suspension was left for one week, and then filtered out to be used for corrosion tests. This electrolyte presented a pH of 5. Testing device was composed of an EGG 273 potentiostat and a 1-liter cell, in which the three electrodes were immersed: a calomel reference electrode saturated in KCl (SCE), a large graphite counter electrode and the specimen as the working electrode. To obtain information relative to a long-term degradation, polarization tests were conducted after a 24-hour immersion. Open circuit potential was controlled throughout the experiment to assess the evolution of the electrochemical state of the surface. Polarization curves were recorded after a one-day immersion at a scan rate of 10 mV/min, starting from –100 mV to finish at +600 mV with respect to the corrosion potential. To correlate electrochemical results with the microstructure of nitrided steels, a *post-mortem* analysis of the corroded surface was performed using a FEG-SEM Zeiss 55 apparatus.

Table 1
Chemical composition of the 90CrMoV8 steel (wt.%).

C	Si	Mn	Cr	Mo	V	Fe
0.5	1.0	0.5	8.0	1.5	0.5	88

3. Results and discussion

3.1. Mechanical and structural properties

3.1.1. Effect of the nitriding process duration realized at 500 °C was studied

Fig. 1a shows the cross section SEM of the steel sample nitrided at 500 °C for 10 h after etching with Vilella's reagent and Vickers micro hardness profiles at different nitriding process times. A variation in the size of micro-indentations is observed which indicates an evolution of hardness with respect to the depth inside the bulk of the material. It is noteworthy that the first indentation was not taken into account because of edge effect. On sub-surface, hardness was found to be around 1250 (10 and 12 h) or 1050 (6 and 8 h) HV while the bulk is characterized by much lower values of about 650 HV. As expected, a significant hardening was thus induced by the plasma nitriding process. Whatever the treatment time, a huge mechanical reinforcement of the surface is achieved with a more than 400 HV hardening. Additionally, due to time-enhanced diffusion processes, the treatment duration parameter has a significant influence on the thickness of the transformed layer. Indeed, it can be estimated from the hardness depth profile that the hardened layer thickness varied from approximately 40 to 120 μm when the treatment duration changed from 6 to 12 h respectively. Thus, as expected, a longer treatment induces a significantly thicker hardened layer, which should be beneficial for the wear resistance. Moreover, another result to highlight is the progressive decrease of hardness with depth (except for the 6 h duration leading to a sharp diffusion layer of only 40 μm thick). Therefore, there is no sharp mechanical discontinuity between the hard layer and the bulk, as in the case of PVD coatings where this drawback can induce their sudden flaking in service.

EDS microanalyses permitted to determine comparative nitrogen contents from the surface to the core of the samples nitrided at 500 °C at 6, 8, 10 and 12 h. As expected, EDS microanalyses reveal that the nitrogen content progressively decreased from the surface towards the bulk (Fig. 1a). This is well correlated with the hardness profile (Fig. 1b, 500 °C – 10 h): top layer is rich in nitrogen (around 15 at.%), which allows the formation of the hard sub-surface layer, whereas for the inner layer, nitrogen enrichment continuously decreases corresponding to the diffusion layer. Even at a 120 μm-depth, steel remains influenced by the hardening treatment. Such similar N-enrichment evolution was obtained for all samples nitrided at 500 °C for the different process durations. The highest nitrogen content measured

on sub-surface associated to the hardest layer was found for the sample nitrided at 500 °C for 10 h.

Microstructure of the modified layer appears on Fig. 1a presenting a SEM cross section of the steel nitrided 10 h at 500 °C. Indeed, the diffusion layer is composed of a thick outer compound layer (of around 45 μm) characterized by a rather diffuse interface with the second inner layer (around 45 μm thick of hardened bulk), starting from this interface and extending towards the bulk material. The highest hardness values correspond to the external layer, while the progressive hardness decrease is due to the softer diffusion layer. Besides, we can underline that whatever the considered nitrided sample no traces of white layer are detected.

Moreover, influence of the nitriding temperature (460, 500 and 520 °C) on the surface hardening was investigated for steel treated at a given process time of 10 h. Fig. 2a shows the SEM cross section of the steel sample nitrided at 460 °C for 10 h together with the results of Vickers micro hardness profiles for the different process temperatures (Fig. 2b). Whatever the temperature, a huge mechanical reinforcement of the surface is achieved with a more than 400 HV hardening. Influence of the temperature is obvious: for only 460 °C, a very thin hardened layer (40 μm-thick) is obtained with a hardening of around 1150 HV. Even if the mechanical reinforcement in these nitriding conditions can be considered as high, the thickness of the diffusion layer is nevertheless too low to withstand the severe wear like abrasion involved in wood machining.

SEM micrograph reveals the same diffusion layers observed above: an outer compound layer and an inner hardened bulk material (Fig. 2a). In the case of the sample nitrided at 460 °C, the diffusion layer is composed of a compound layer of around 20 μm thick and a hardened bulk material of the same thickness. Besides, steel nitrided at 460 °C shows a sharp mechanical discontinuity between the hard layer and the bulk which may induce a negative effect under mechanical strains. Nitriding at 520 °C, the top-surface is less hard than the one nitrided at 500 °C and above a 100 μm depth the micro hardness measured drops at 300 HV. This can be interpreted by a modification of the bulk material itself only tempered at 530 °C.

According to the previous results, the optimal nitriding parameters seem to be a temperature of 500 °C for a treatment time of 10 h.

To verify this assumption, the crystallographic nature of the different samples was analyzed by XRD (Fig. 3). XRD pattern of the untreated material reveals the characteristic diffraction peaks of iron: (110) at 51.6°, (200) at 76.1° and (211) at 98.7°. When we fixed the nitriding temperature to 500 °C and varied the process duration from 6 to 12 h (Fig. 3a) we can see the typical phases formed after the nitriding process.

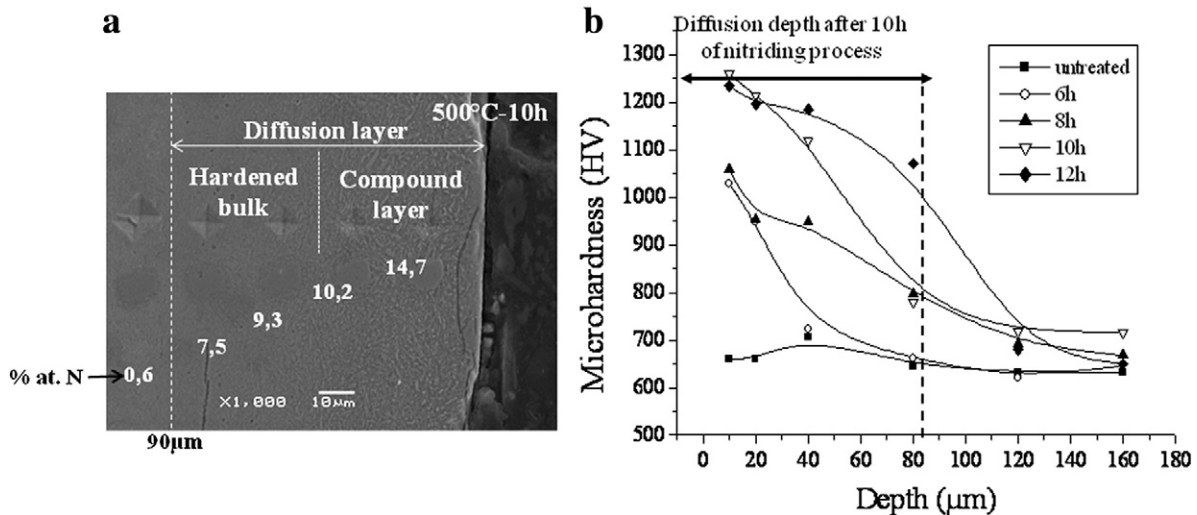


Fig. 1. (a) SEM cross section observation and N content for the steel nitrided at 500 °C for 10 h, and (b) hardness profiles vs sample depth for nitrided steels at 500 °C for different times.

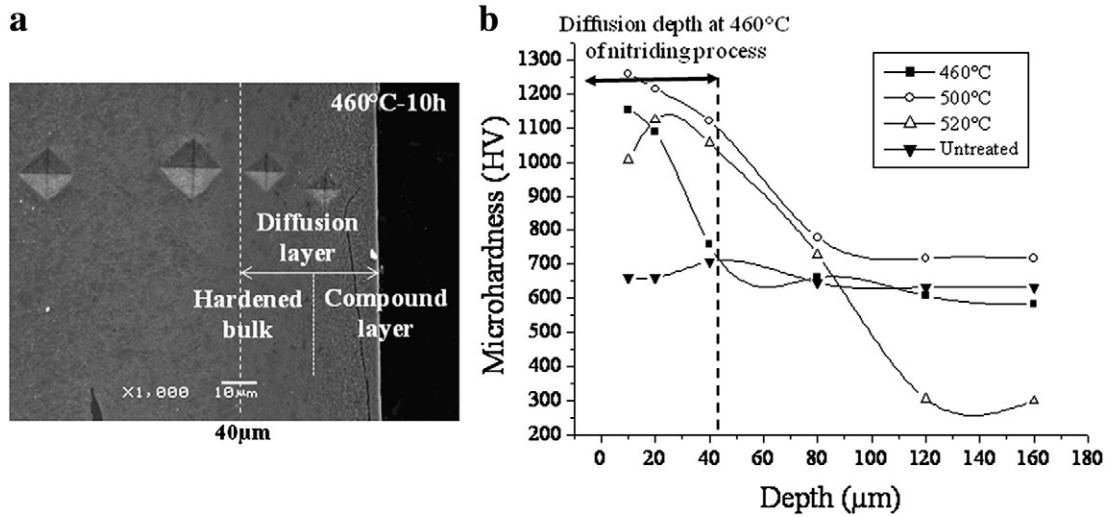


Fig. 2. (a) SEM cross section observation for the steel nitrided at 460 °C for 10 h, and b) hardness profiles vs sample depth for nitrided steels at different temperatures for 10 h.

The first observation of these patterns reveals that whatever the treatment duration, the Fe (110) peak attributable to iron is widened and shifted towards the lower angles with respect to untreated steel ones (50° instead of 51.6°) while the two other XRD peaks of Fe, (200) and (211) completely disappeared. This suggests that nitrogen is

introduced into the solid solution, generating internal stresses, which should contribute to a higher fatigue resistance as commonly accepted for nitriding processes. Considering the evolution of iron nitrides peaks with the treatment duration, it can be concluded that longer treatments favor their growth and crystallized character as reflected by the intensity and narrowness of peaks respectively. As for the Fe (110) peak, all the iron nitride peaks are shifted to lower angles when we increase the process duration. Iron nitrides detected are ϵ and γ' (Fe_{2-3}N and Fe_4N respectively): after the 6 hour-treatment, a well crystallized γ' (111) orientation at 46.9° is only present as minor γ' (200) at 54.6°, ϵ (100) at 43.8° and ϵ (110) at 81.1°. When we increased the duration treatment to 8 h, the γ' (111) and (200) diffraction peaks are still present but with lower intensity as the ϵ ones. For longer treatments (10 and 12 h), broad γ' (111) and (200) diffraction peaks can be observed. Besides, we still detect the ϵ (100) and (110) with higher intensities than those at 6 h, and a broad ϵ (102) at 66.2°, ϵ (103) at 90.4° and ϵ (112) at 100° appeared. Consequently, the ϵ phase seems to be predominant with a total peaks area apparently equal or even higher than that of γ' (111) and (200).

It is noteworthy that no traces of chromium nitride, that would be harmful from a corrosion protection point of view, were observed. Furthermore, it can also be noticed that the relative amount of ϵ increases with the treatment duration. This result again would be promising for corrosion protection insofar as it is known that ϵ -based nitrided layers might induce a passive character [15].

Then we fixed the nitriding duration to 10 h and varied the process temperature from 460 to 520 °C (Fig. 3b). The first observation of these patterns reveals that whatever the process temperature, the Fe (110) peak attributable to iron is widened and shifted towards the lower angles with respect to untreated steel ones (49.9° instead of 51.6°) while the two other XRD peaks (200) and (211) completely disappeared. Besides, for all treatments, XRD patterns are very similar which reveals that the temperature is less influent on the nitrided layer crystallinity than the treatment duration. As for Fe (110) peak, all the iron nitride peaks are shifted to lower angles for nitriding performed at higher temperatures. We still observe the γ' (111) at around 46.8° and (200) at 54.2° diffraction peaks. The crystallinity of the γ' phase decreases when the process temperature increases. Furthermore, the ϵ phase is always detected with five diffraction peaks: (100) at around 43.7°, (102) at 66.3°, (110) at 81.1°, (103) at 90.5° and (112) at 100°. It can be noticed that the ϵ phase diffraction peak intensity increased with the temperature and is the highest and most defined at 500 °C. As previously observed for the highest temperatures, the ϵ phase seems to be predominant.

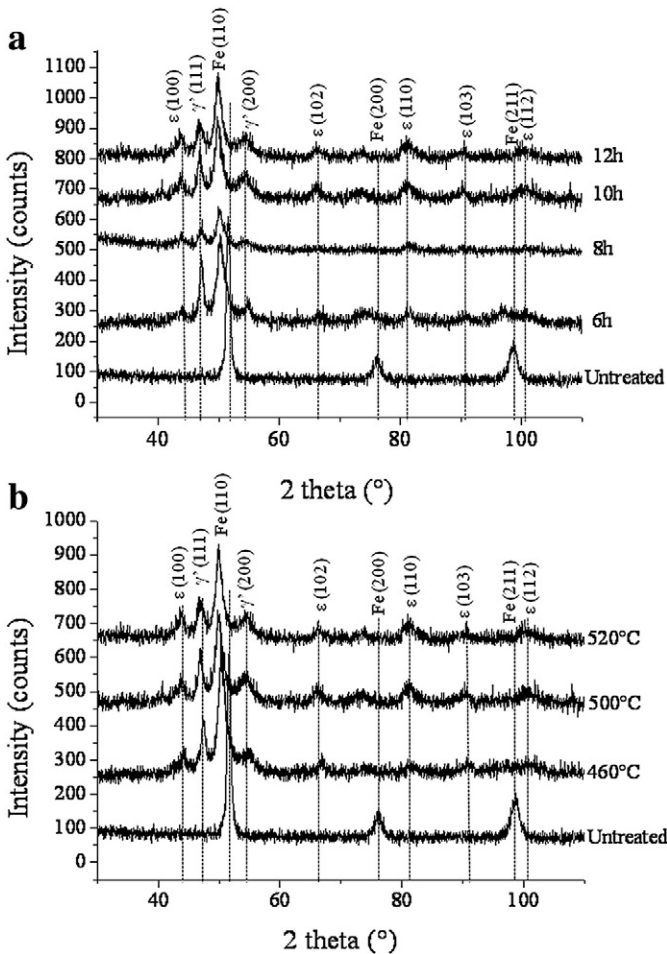


Fig. 3. (a) XRD patterns of untreated and nitrided 90CrMoV8 steel samples at 500 °C for 6, 8, 10 and 12 h, and (b) XRD patterns of untreated and nitrided 90CrMoV8 steel samples at 460, 500 and 520 °C for 10 h.

To sum up, it is noteworthy that the optimal nitriding conditions deduced from the mechanical investigations (500 °C for 10 h), also led to the desired microstructure characterized by a high amount of ϵ nitride.

3.2. Corrosion behavior

The previous part of the paper identified the temperature of 500 °C as the nitriding temperature leading to a thick and hard enough layer, which is a prerequisite for a tool to withstand the severe wear involved during machining operations. Nevertheless, in the case of wood materials, a hardened tool surface cannot be considered as a sufficient condition. Indeed, tools employed in wood machining may induce a further potential degradation mode linked to the subsequent release of a tannin-based potentially aggressive solution. Such a physico-chemical investigation has never been proposed in the literature, especially regarding nitrided steels. The liquid susceptible to be oozed out during machining, named “wood juice” cannot be synthesized and is prepared by infusion in water, for one week, of wood veneers.

In order to obtain a thick enough layer and for mechanical property reasons, the corrosion study will be focused on the 500 °C treatment series. Moreover, this temperature is constituent with those recommended by Gontijo et al. [21] to preserve the passive character of the 304 L stainless steel.

Fig. 4 shows the effect of the treatment duration at the constant process temperature of 500 °C on the electrochemical behavior. In order to assess the long-term evolution of the kinetic of degradation, polarization curves were recorded after a one-day immersion time. Moreover, both thermodynamic and kinetic parameters deduced from these curves are gathered in Table 2.

It is first noteworthy that, despite a rather low chromium content, untreated steel in contact with the specific wood machining simulating solution behaves as a passive material, characterized by a high corrosion potential value (−307 mV/ECS), a very low corrosion rate (~ 37 nA/cm²) associated with a wide passive domain of about 250 mV. Whatever the treatment time, the electrochemical potential of all nitrided parts is significantly shifted towards negative values, in relation with the modification of the metallic interface by the presence of nitrides. From a thermodynamic point of view, this less noble character of the exposed surface should lead to a more reactive material. Indeed, corrosion rates are one decade higher. Nevertheless, they remain at a very low level, far lower than those conventionally encountered with tool steels put in contact of aggressive media (some

Table 2
Electrochemical parameters of the different samples deduced from polarization curves.

	Untreated steel	6 h at 500 °C	8 h at 500 °C	10 h at 500 °C	12 h at 500 °C
E_{corr} (mV/ECS)	−307	−559	−569	−582	−575
I_{corr} (nA/cm ²)	37	233	417	392	347
Passive domain extent (mV)	255	87	150	157	156

tens of $\mu\text{A}/\text{cm}^2$ at least in general). In fact, it can be observed that the anodic part of the potentiodynamic curves (for potential above the corrosion potential) is flattened, which is linked to the passive-like nature of the surface. Thus, despite of the heat treatment, the initial passive character of steel is preserved, which is in accordance with the absence of CrN precipitates not detected by XRD [24]. The free chromium in the compound layer is then left at a level high enough to stabilize an efficient protective passive film. However, the extent of the passive domain for treated surfaces is reduced (~ 150 mV), suggesting a potentially higher propensity to pitting corrosion in comparison with the substrate.

Compared to other treatments, the 6 hour nitrided steel shows an unexpected behavior characterized by a significantly shorter passive domain. A deeper analysis of its polarization curve indeed shows a shoulder in the anodic part (see the inset in Fig. 4) suggesting a sharp increase of the dissolution kinetic. SEM observation of the surface after corrosion (Fig. 5) allows us to attribute this shoulder to the development of pitting phenomena (Fig. 5b). Except this local attack, all nitrided steels show a uniform corrosion giving rise to a non-adherent corrosion scale. Obviously, such discontinuous layers cannot protect the material by any barrier effect, which again contribute to explain the low corrosion rates of nitrided surfaces by their intrinsic passive-like nature.

For longer treatments (8, 10, and 12 h, Fig. 5c–e), electrochemical properties are similar (Table 2). However corroded surface of steel treated 12 h has to be distinguished presenting a cracked surface (Fig. 5f). This has to be correlated with the brittle character of the surface characterized by very high hardness values.

Optimal nitriding times at 500 °C are then 8 or 10 h, leading to a moderate passive behavior without propensity to neither crack initiation nor pitting. Such electrochemical behavior results again from the predominance of ϵ nitrides. Moreover, preservation of a passive character is also the direct consequence of the absence of CrN precipitates.

4. Conclusions

Plasma nitriding with a $\text{N}_2\text{-H}_2$ gas mixture (80–20) was found to be a successful process for the enhancement of hardness and hence wear resistance, without losing the intrinsic protectiveness of 90CrMoV8 steel, material base for wood machining tools. It was shown that increasing the treatment time leads to thicker (around 120 μm) and harder (above 1200 HV) nitrided layers. Different iron nitrides were present, as the origin of the great hardening. The ϵ phase was mainly identified and no traces of chromium nitrides were detected in the modified layer. No white layer was observed in the nitrided samples. The temperature has an effect on the morphological properties of the obtained diffusion layers but not on their crystallinity. The optimal nitriding parameters are 500 °C during 10 h according to the structural and morphological analyses.

Electrochemical measurements were performed in an original electrolyte simulating the solution in contact with the tool when wood is machined. The surface is then observed at the SEM scale after the corrosion test. For this “wood juice”, untreated steel behaved as a

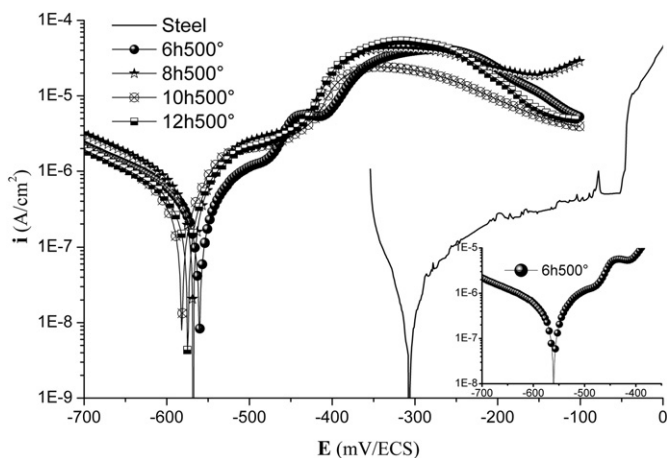


Fig. 4. Polarization curves in “wood juice” electrolyte of the 90CrMoV8 steel before and after nitriding at 500 °C for different treatment times.

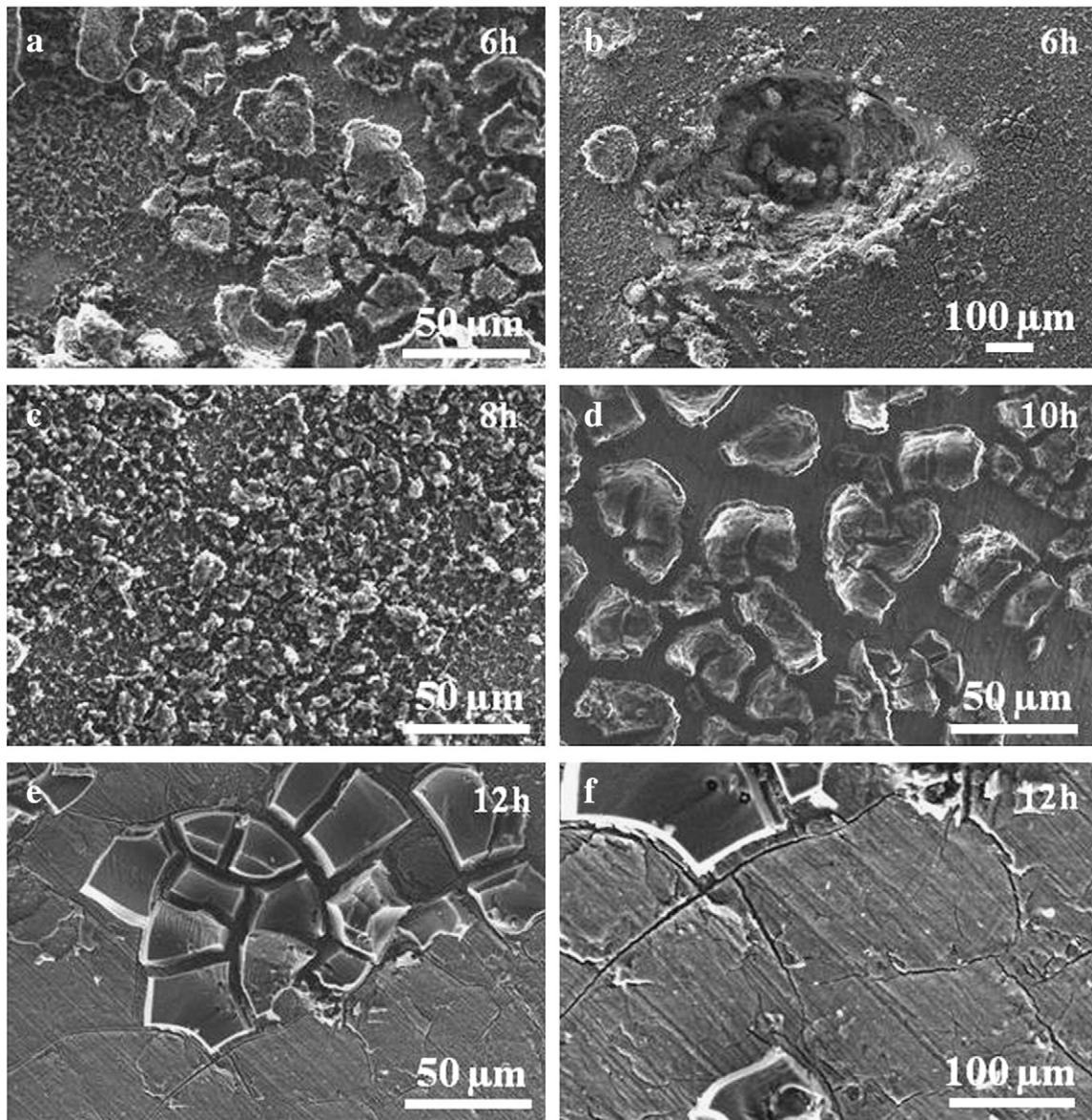


Fig. 5. SEM surface morphology of nitrided steel samples after 24-hour corrosion tests.

passive material. After plasma treatment, the corrosion propensity is higher (potentials more negative and corrosion rates increased) but treated surfaces reveal a passive character owing to the predominance of ϵ phase nitrides and to the absence of CrN precipitates. For too short nitriding times (6 h) surface is subjected to pitting, while for too long treatments (12 h) the corroded surface is cracked. So, it has been shown that long duration treatments are recommended for achieving a thick very hard layer, which is interesting from a tribological viewpoint. Furthermore, owing to the release of potentially aggressive liquids during the wood machining, tools need also to be corrosion resistant. As a conclusion, to combine these two complementary functional properties, plasma nitriding of 90CrMoV8 steel for 10 h at 500 °C is relevant for wood machining applications.

Acknowledgments

The authors wish to thank the Regional Council of Burgundy and EGIDE for their financial support, and also the technical staff of the Arts et Métiers ParisTech of Cluny: especially Denis Bonsembiante for

the nitriding experiments, Romaric Masset and Pierre-Michel Barbier for the sample preparation.

References

- [1] C. Labidi, Ph.D. report n° 58-2006, ENSAM, Cluny, France
- [2] Y.Z. Shen, K.H. Oh, D.N. Lee, *Mater. Sci. Eng. A* 434 (1-2) (2006) 314.
- [3] W.P. Tong, C.Z. Liu, W. Wang, N.R. Tao, Z.B. Wang, L. Zuo, J.C. He, *Scr. Mater.* 57 (2007) 533.
- [4] J.R. Roth, *Industrial Plasma Engineering, Volume 1: Principles*, IOP Publishing Ltd, Bristol, 1995.
- [5] M. Ohring, *The Material Science of Thin Films*, Academic Press, San Diego, 1992.
- [6] T. Michler, *Surf. Coat. Technol.* 202 (2008) 1688.
- [7] L. Wang, Y. Li, X. Wu, *Appl. Surf. Sci.* 254 (20) (2008) 6595.
- [8] P. Schaaf, *Prog. Mater. Sci.* 47 (1) (2002) 1.
- [9] G. Simon, M.A.Z. Vasconcellos, C.A. dos Santos, *Surf. Coat. Technol.* 102 (1998) 90.
- [10] V.A. Alves, C.M.A. Brett, A. Cavaleiro, *Surf. Coat. Technol.* 161 (2-3) (2002) 257.
- [11] M.A.M. Ibrahim, S.F. Korablov, M. Yoshimura, *Corros. Sci.* 44 (4) (2002) 815.
- [12] A.-S. Loir, D. Pech, P. Steyer, Y. Gachon, C. Héau, J.-C. Sanchez-Lopez, *Plasma Processes Polym.* 4 (2) (2007) 173.
- [13] L. Chekour, C. Nouveau, A. Chala, M.A. Djouadi, *Wear* 255 (7-12) (2003) 1438.
- [14] A. Chala, L. Chekour, C. Nouveau, C. Saied, M.-S. Aida, M.-A. Djouadi, *Surf. Coat. Technol.* 200 (1-4 SPEC. ISS) (2005) 512.
- [15] P. Steyer, J.-P. Millet, J.-P. Peyre, P. Jacquot, D. Hertz, *Surf. Eng.* 19 (3) (2003) 173.

- [16] M.L. Doche, V. Meynie, H. Mazille, C. Deramaix, P. Jacquot, *Surf. Coat. Technol.* 154 (2–3) (2002) 113.
- [17] L. Pranevicius, C. Templier, J.-P. Rivière, P. Méheust, L.L. Pranevicius, G. Abrasonis, *Surf. Coat. Technol.* 135 (2–3) (2001) 250.
- [18] Y.-T. Xi, D.-X. Liu, D. Han, *Appl. Surf. Sci.* 254 (18) (2008) 5953.
- [19] M. Olzon-Dionysio, S.D. de Souza, R.L.O. Basso, S. de Souza, *Surf. Coat. Technol.* 202 (15) (2008) 3607.
- [20] M. Esfandiari, H. Dong, *Surf. Coat. Technol.* 201 (14) (2007) 6189.
- [21] L.C. Gontijo, R. Machado, S.E. Kuri, L.C. Casteletti, P.A.P. Nascente, *Thin Solid Films* 515 (3) (2006) 1093.
- [22] L. Nosei, S. Farina, M. Avalos, L. Nachez, B.J. Gomez, J. Feugeas, *Thin Solid Films* 516 (2008) 1044.
- [23] S.D. de Souza, M. Kapp, M. Olzon-Dionysio, M. Campos, *Surf. Coat. Technol.* 204 (18–19) (2010) 2976.
- [24] S. Valette, P. Steyer, L. Richard, B. Forest, C. Donnet, E. Audouard, *Appl. Surf. Sci.* 252 (13 SPEC. ISS) (2006) 4696.